國立交通大學

資訊科學與工程研究所

碩 士 論 文

針對 BRDF 的全域光源重要性採樣方法之研究

An Efficient BRDF Importance Sampling Method

for Global Illumination

研 究 生：翁士欽

指導教授：施仁忠 教授

中 華 民 國 九 十 五 年 六 月

針對 BRDF 的全域光源重樣性採樣方法之研究
An Efficient BRDF Importance Sampling Method for Global Illuimation

研 究 生：翁士欽　　Student：Shr-Ching Weng

指導教授：施仁忠　　Advisor：Zen-Chung Shih

國 立 交 通 大 學
資 訊 科 學 與 工 程 研 究 所
碩 士 論 文

A Thesis

Submitted to Institute of Computer Science and Engineering

College of Computer Science

National Chiao Tung University

in partial Fulfillment of the Requirements

for the Degree of

Master

in

Computer Science

June 2006

Hsinchu, Taiwan, Republic of China

中華民國九十五年六月

針對 BRDF 的全域光源重要性採樣方法之研究

研究生: 翁士欽　　　　　　　　　　指導教授: 施仁忠 教授

國立交通大學資訊科學與工程研究所

摘要

我們藉由球面輻射基底函數(SRBF)的特性，針對雙向反射分佈函數(BRDF)提出一種新的重要性採樣方法。我們經由實驗證實，透過非線性最佳化的演算法,將雙向反射分佈函數轉換至球面輻射基底函數的表示形式之誤差是在一個可容忍的誤差範圍內。此外，根據球面輻射基底函數的表現形式，我們也提出一種有效率的重要性採樣方法,其產生出來的採樣分佈可以契合球面輻射基底函數所描述的資料分佈，此方法可以在全域光源照射的環境下，有效率地繪製包含多種複雜材質的場景影像。

An Efficient BRDF Importance Sampling Method

for Global Illumination

Student: Shr-Ching Weng   Advisor: Prof. Zen-Chung Shih

Department of Computer Science

National Chiao-Tung University

ABSTRACT

We present a new technique for sampling the importance of realistic bidirectional reflectance distribution function (BRDF) models by using spherical radial basis functions (SRBFs). We demonstrate that the measured BRDF data can be represented in SRBFs in a tolerated error bound by using our non-uniform and non-negative SRBF fitting algorithm. Then, we present an efficient sampling algorithm on the unit sphere, and the generated point distribution can match the SRBF representation. We are capable of creating images with multiple measured BRDFs under global illumination.

Acknowledgements

I would like to express my sincere gratitude to my advisor, Prof. Zen-Chung Shih, who provided support and encouragement in these days. I deeply appreciate his patient instruction and guidance. Then, I would like to thank all the members in Computer Graphics and Virtual Reality Laboratory for their help and suggestions. Especially, I gratefully acknowledge the helpful discussions with Yu-Ting Tsai on several points in the thesis. Moreover, I want to thank all the people who ever helped me during these days. Finally, I'm indebted to my parents for their love, support and encouragement over the years. I would like to dedicate my achievement to my dear parents.

Contents

Figure List

Chapter 1

Introduction

The bidirectional reflectance distribution function (BRDF) describes how light is reflected at the material's surface. The analytical BRDF model, such as Phong model [17] or Cook-Torrance [4], is hard to describe a material with complex scattering behavior. In order to improve the quality of realistic images with a wide range of BRDFs, more and more researches focus on efficient rendering with measured BRDF data. However, there is a major challenge in the Monte-Carlo based global illumination approach incorporating with complex BRDF models - the sampling efficiency. When tracing each ray in the scene, the tracing path of the ray is desired to be selected by the importance distribution of the BRDF as much as possible. Take a highly specular material for example, the most part of incident energy are gathered in the specular direction with a fixed outgoing direction. It would waste lots of samples if we generate samples randomly or uniformly. In this situation, only few sampling paths get the intensity. On the other hand, if we could generate samples against the specular direction, it would reduce the image variance and increase the efficiency of rendering. Therefore, how to find the importance sampling direction with BRDF plays a critical role in efficient realistic image rendering.

In order to analyze the original measured BRDF data to find the probability distributions of sampling directions, many researchers transform original data into other representation forms (wavelet [12] [14] [2], factored representation [13], … etc), then generate sampling directions according to the probability distribution found in the specified representation. The concept of our approach is the same as previous researches. We choose spherical radial basis functions (SRBF) to represent the measured BRDF data, then find the distribution on the unit sphere, render the image against the distribution finally.

1.1 Motivation

Special radial basis functions (RBFs) defined on the unit sphere are called spherical radial basis functions (SRBFs) by Narcowich and Ward [15]. Since SRBFs are defined in the spherical domain, there are some intrinsic potential make SRBF more appropriate to represent the spherical data, such as BRDF data. First, owing to the SRBFs are defined in spherical domain, we can directly fit our model to the data without reparameterization. Therefore, we could avoid the inaccuracy probably produced from the reparameterization process. Second, the convolution of two SRBF kernels in some situations has a simple mathematical form, thus we can use this property to calculate the integral for probability estimation without extra processes to construct the probability density function (PDF). Third, using scattered SRBFs, we can represent the original data with few memory storages, and the approximated results are in a tolerated error bound.

According to the useful properties of SRBFs described above. We can use SRBF to represent the BRDF data without reparameterization when fitting SRBFs to the

BRDF measurements. Additionally, the approximated results are accurate enough to represent most features of the original data, and we can directly estimate the probability for importance sampling with the simple from of convolution by choosing the appropriate SRBF kernels. The potential benefits of SRBFs would make the importance sampling more efficient.

1.2 Overview

The goal of this thesis is to demonstrate that the scattered SRBFs are appropriate to represent the measured BRDF data of complex materials. With some useful properties of SRBF, we can easily apply the resulting representation in the Monte Carlo importance sampling technique. Finally, we show that the efficiency of BRDF importance sampling can be improved with our sampling scheme.

1.3 Thesis Organization

The following chapters are organized as follows. In Chapter 2, we will review the researches about the representations for complex BRDF models and the BRDF importance sampling strategies based on each different representation. In Chapter 3, we introduce the background of SRBFs and the advantages of scattered SRBFs. Then, in Chapter 4, we will describe how we fit scattered SRBFs to the measured BRDF data, and how we generate sample directions at run-time efficiently. The implementation and results will be demonstrated in Chapter 5. Finally, the conclusions and future work are given in Chapter 6.

Chapter 2

Related Work

The goal of global illumination is to solve the rendering equation which is first formulated by Kajiya [8]:

$$L(x,\omega_o) = L_e(x,\omega_o) + \int_\Omega \rho(x,\omega_i,\omega_o) L_i(x,\omega_i)(\omega_i \cdot n) d\omega_i \,, \tag{1}$$

where L_i is the incident radiance, and ρ is the BRDF . Monte Carlo approaches are used to solve the integrals which have no analytical or numerical solution, such as the rendering equation. They solve the integrals by computing the average of random samples of the integrand, accumulating these values and taking the average. Importance sampling technique is a variance reduction technique of Monte Carlo approaches. Most Monte Carlo approaches use importance sampling of either ρ or L_i to solve the rendering equation. When sampling the light source for direct illumination, there are some sampling methods have been demonstrated [1] [3] [9]. However, these methods are hard to deal with the complex materials measured from the real-world, and it's not practical to pre-compute the incident radiance at all points in the scene in general case of global illumination. Thus, we attempt to sample according to the measured BRDF ρ.

In the remainder of this chapter, we will first describe two mainstreams of the BRDF models, and their abilities to be applied to importance sampling technique. Then we briefly introduce several representations for BRDF proposed by previous researchers, and how they perform importance sampling based on their representation.

2.1 BRDF Models

BRDF models used generally nowadays can be classified into two mainstreams: one is *phenomenological-based* models, and the other is *data-measured based* models.

Phenomenological-based BRDF models are usually expressed in an analytical formula that attempt to describe the qualitative properties of real-world surfaces. The popular Phong shading model [17] belongs to this category, and other physically-based models [4] [7] which can capture the Fresnel reflection, rough microgeometry or other physical effects are also part of this. These models tend to use some intuitive parameters to modify their reflection behavior. It is easy to evaluate the value for rendering. Nevertheless, they are hard to describe the materials with complex behavior, even though they succeed to describe the complicated physical phenomenon. Sometimes they are difficult to be applied to importance sampling, since the analytic formula may be difficult or impossible to integrate and invert to estimate the probability distribution for sampling.

Data-measured based models are unlike the phenomenological-based models, their reflection distribution properties of real-world surfaces are measured practically. These models sometimes are used in tabular form for rendering directly. Once in a while, in order to analyze the original measured data, the model may be represented in the form constructed by wavelets, factorized matrix, or other data analyzing approach. The quality of these representations depends on not only the accuracy of the measurements but also the approximation performance.

2.2 BRDF Importance Sampling

BRDF importance sampling is a technique to reduce the image variance in physically-based rendering. Its concept is to find the distribution based on the representation of BRDF. Shirley demonstrated how to sample the traditional Phong BRDF model efficiently [19], Lafortune also presented importance sampling schemes for the modified Phong model [11]. Ward [22] showed the stochastic sampling method for the BRDF models composed of (elliptical) Gaussian kernels. For more examples, please see Pharr and Humphreys [16].

Lafortune [10] used multiple cosine-lobes for representing the BRDF, he used non-linear fitting algorithm to fit sums of cosine-lobes to an analytical model or to actual measurements. Though this representation is simple and can be applied for Monte Carlo importance sampling efficiently, it is hard to approximate the complex BRDF by using his fitting process.

Lalonde [12] used wavelets to represent the BRDF and proposed an importance sampling scheme by binary searching the tree constructed against the coefficients of each wavelet basis. Matusik [14] also used a wavelets representation of BRDF, and he presented a numerical sampling method based on wavelets analysis.

Lawrence et al. [13] demonstrated an importance sampling method based on a factored representation. They reparameterized the BRDF by using half-angle [18], then used non-negative matrix factorization (NMF) twice to decompose the BRDF data for efficient importance sampling.

Our approach represents the BRDF using scattered SRBFs. Tsai and Shih [20] have shown this representation performs better than wavelets in data analysis. Furthermore, we can directly fit scattered SRBFs to the BRDF data without reparameterization. We also propose an efficient importance sampling method based on this representation. In the following chapters, we will describe how we represent the measured BRDF data with scattered SRBFs and how we estimate the probability distribution for importance sampling.

Chapter 3

Spherical Radial Basis Functions

Spherical radial basis function (SRBF) is a special radial basis function (RBF) defined on the unit sphere. SRBFs avoid distortions and the artificial boundaries when they are used to analyze the data on sphere. In this chapter, we first introduce the background of SRBFs, and express the useful properties of SRBFs that had been developed by previous researchers. Then we discuss the scattered SRBFs briefly, and point out the advantages of scattered SRBFs.

3.1 Background of SRBFs

SRBF is recognized as an axis-symmetric reproducing kernel function defined on $\mathbb{S}^m$, the unit sphere embedded in $\mathbb{R}^{m+1}$. It can be taken as a special radial basis function (RBF) defined on the unit sphere, i.e. the kernel functions only depend on the spherical distance between unit vectors (Figure 3.1).

Let η and ξ be two points on $\mathbb{S}^m$, and let $\theta(\eta,\xi)$ be the geodesic distance between η and ξ on $\mathbb{S}^m$, i.e. the arc length of the great circle joining the η and ξ. Because kernel functions of SRBF are depending on θ, and SRBF can be expressed in the expansions of Legendre polynomials:

$$G(\cos\theta) = G(\eta \cdot \xi) = \sum_{l=0}^{\infty} G_l P_l(\eta \cdot \xi), \qquad (2)$$

where $P_l(\eta \cdot \xi)$ is the Legendre polynomials of degree *l*, and the coefficients G_l of each Legendre polynomial satisfy the following conditions:

$$\begin{cases} G_l \geq 0 \\ \sum_{l=0}^{\infty} G_l < \infty \end{cases}$$

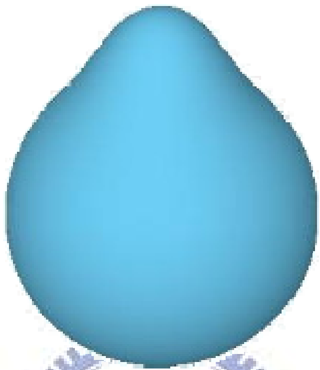

Figure 3.1: 3D plot of a Gaussian SRBF

When all G_l are positive, a spherical function $F(\eta)$ can be represented in SRBF expansions:

$$F(\eta) = \sum_{k=1}^{N} F_k G(\eta \cdot \lambda_k) \qquad (3)$$

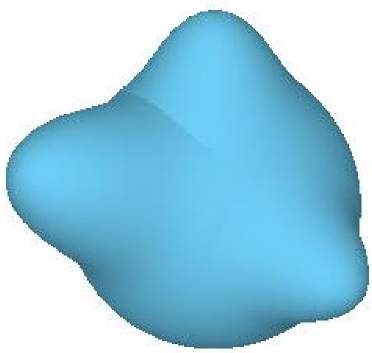

Figure 3.2: Represent $F(\eta)$ with SRBF expansions.

Since SRBF has expansions of the Legendre polynomials, there is a very useful property based on the orthogonal property of Legendre polynomials in [-1, 1] called *spherical singular integral*

$$\int_{\mathbb{S}^m} G(\eta \cdot \xi_g) H(\eta \cdot \xi_h) d\omega(\eta) = \sum_{l=0}^{\infty} G_l H_l \frac{\omega_m}{d_{m,l}} P_l(\xi_g \cdot \xi_h) \tag{4}$$

where ω_m is the total surface area of $\mathbb{S}^m$, $d_{m,l}$ is the dimension of the space of order-l spherical harmonics on $\mathbb{S}^m$, and $d\omega$ denotes the differential surface element on $\mathbb{S}^m$.

The spherical singular integral could be transformed into a simpler form in some conditions. Tsai and Shih [20] have proved that the convolution of two Abel-Possion SRBFs kernels, or two Gaussian SRBFs kernels has a mathematically simple form with small *m*. For example, the definition of Gaussian SRBF kernel is

$$G^{Gau}(\eta \cdot \xi; \lambda) = e^{-\lambda} e^{\lambda(\eta \cdot \xi)}, \quad \lambda > 0, \tag{5}$$

where λ, the parameter called bandwidth, describes the coverage of the SRBF, and the convolution of two Gaussian SRBFs can be written as

$$G^{Gau} *_m H^{Gau}(\xi_g \cdot \xi_h; \lambda_g, \lambda_h) = e^{-(\lambda_g + \lambda_h)} \omega_m \Gamma(\frac{m+1}{2}) I_{\frac{m-1}{2}}(\|r\|)(\frac{2}{\|r\|})^{\frac{m-1}{2}} \tag{6}$$

where $r = \lambda_g \xi_g + \lambda_h \xi_h$. For more details about the proof of the equation, please refer to [20], and there are two references for further about SRBF [15] [6].

3.2 Scattered SRBFs

Distribution of the SRBFs' centers on the sphere affects the compression efficiency significantly. If we use uniform SRBFs to represent the data with sparse distribution, it would waste lots of basis kernels on the region without any data. On the other hand, using scattered SRBFs, i.e. adapting the center, bandwidth and coefficient of each basis, we can locate the SRBF kernels based on the data distribution on the sphere. Therefore, scattered SRBFs can capture the feature of the original data with much fewer bases than those used in uniform SRBFs. Nevertheless, it may be hard to compute the parameters of each scattered SRBF (i.e. center, bandwidth, and coefficient) from original data. Fortunately, Tsai and Shih [20] present a novel approach to fit data with scattered SRBFs recently. Their approach makes scattered SRBFs more practical for representing data on sphere.

Chapter 4

Sampling Scheme

Our system consists of two major processes, one is the off-line process and the other is the run-time rendering process. In the off-line process, we transform the BRDF measurements into the scattered SRBF representation. In the run-time rendering process, we first determine how many samples should be taken from each SRBF. Then we generate samples based on the probability density function (PDF) calculated from each SRBF. Finally, we combine the sampling results with *multiple importance sampling* technique presented by Veach and Guibas [21].

The following sections are organized as follows. In Section 4.1, we will introduce the non-uniform and non-negative SRBF fitting algorithm which we use to transform the measured BRDF data into scattered SRBFs, and discuss the initial guess applied for BRDF data. In Section 4.2, we first briefly introduce the *multiple importance sampling* technique. Then, we describe how to determine the number of samples of each SRBF kernel and how to generate samples from each SRBF kernel.

4.1 Off-line Process

In this section, we would show how to represent the measured BRDF data by using scattering SRBFs. We first introduce the fitting algorithm, and then we describe the initial guess for BRDF data in the fitting process.

4.1.1 Non-uniform and non-negative SRBF fitting algorithm

We now describe how we transform the original BRDF measurements into the scattered SRBFs representation. The measured BRDF data are usually represented in tabular form, row is the outgoing (viewing) direction, and column is the incident (lighting) direction. When we fix one outgoing direction, we can get a vector which describes the ratio of energy from all incident directions (Figure 4.1). The order of each element contained in the vector is the same as the pixel order defined in the cubic texture, i.e. first unfold each face's pixels into a vector, then concatenate the unfolded vectors of each face in the order +x, -x, +y, -y, +z, -z.

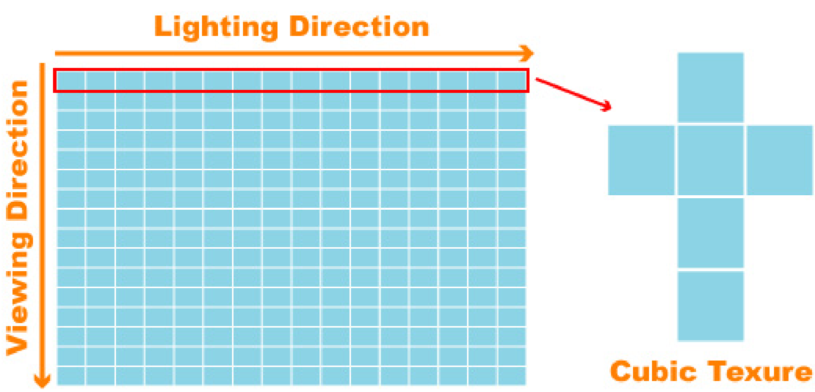

Figure 4.1: The format of measured BRDF data.

In our fitting process, we fit the scattered SRBFs to the data in a vector of each outgoing direction respectively, and there are three sets of parameters we want to optimize: the set of coefficients L, the set of centers Ξ_2, and the set of bandwidth parameters Λ_2. Our objective is to minimize the square error with the original data:

$$\begin{aligned}&\{L, \Xi_2, \Lambda_2\} = \underset{\{L, \Xi_2, \Lambda_2\}}{\arg\min} \int_{\mathbb{S}^2} \left| \rho_{\omega_o}(\omega_i) - \tilde{\rho}_{\omega_o}(\omega_i) \right|^2 d\omega(\omega_i), \\ &\tilde{\rho}_{\omega_o}(\omega_i) = \sum_{k=1}^{n_l} L_k G(\omega_i \cdot \xi_{2,k}; \lambda_{2,k})\end{aligned} \tag{7}$$

Tsai and Shih [20] have presented a novel method to solve this objective function when modeling the lighting environment. In their fitting approach, the coefficients of each kernel basis are calculated by *ordinary least-squares* (OLS) or *regularized least-squares* (RLS). However, fitting by OLS or RLS would make the coefficients become negative in some situations. Because we need to use the coefficients to estimate the probability distribution, we must constrain all coefficients to be positive. Therefore, we also use L-BFGS-B solver [23] to fit the coefficients instead.

The fitting process composes of three main steps:

1. Using L-BFGS-B solver to optimize the set of centers with a given initial guess or the temporary results of the previous iteration.
2. Then, using L-BFGS-B to solve the set of bandwidth parameters and the set of coefficients in turn.
3. If the squared difference errors between current and previous iteration are less than a threshold, the process is terminated. If the count of iterations exceeds a user-defined threshold, break the process as well.

This fitting process is one kind of non-linear optimization. The fitting results are highly dependent on the initial guess. In other words, the initial guess would dominate the accuracy of the representation. In next subsection, we would introduce the initial guess for BRDF data in more details.

4.1.2 Initial Guess for Non-linear Optimization of BRDF data

As mentioned in last subsection, the initial guess plays an important role in non-linear optimization. Tsai and Shih [20] have studied this problem recently, and they present a reasonable guess based on some heuristics to decrease approximation errors. The principle of their initial guess is to make the initial centers of each kernel basis locate at all local peaks of the original data as close as possible, and to estimate a reasonable bandwidth according to the coverage of each initial center. Based on this principle, they generate lots of candidate guesses sorted by the coverage-weighted intensity, and then attempt to choose guesses which avoid the initial centers gathering in local area. This guessing scheme works well for the data with high dynamic range (HDR) property. While for most BRDFs data, the magnitude of the gradient of each data element is much smaller than the HDR image. In order to apply this guessing schema for BRDF data to achieve the same performance in HDR image, we only need to do a minor change – emphasizing the weighting of intensity. We do this straight by squaring the influence of intensity. This modification makes this initial guess schema much tend to select the candidates with high intensity in the entire region of BRDF.

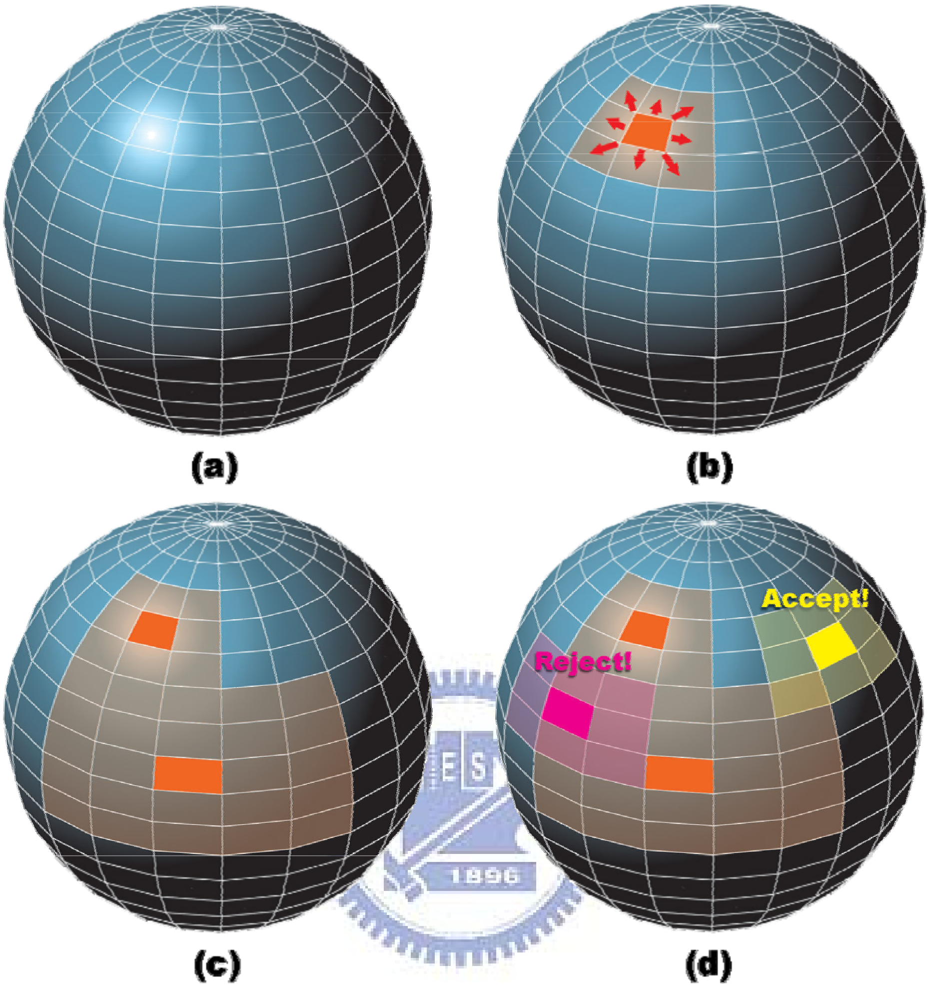

Figure 4.2: Overview of initial guess generation.

(a) Visualization of measured BRDF data on unit sphere.
(b) Estimate the coverage of each unit direction on the sphere.
(c) The candidates selected so far and the summation of their coverage (i.e. the area colored with light orange).
(d) The candidate falls within the range (c) would be rejected (magenta one), yet would be accepted (yellow one).

Figure 4.2 gives the overview of the initial guess. The original measurements of BRDF are discrete. After mapping the measured data onto the sphere, we can get the visualization result (a). Then we estimate the coverage of each direction in a dense set of unit directions, i.e. each data element on the sphere, as illustrated in (b). With each unit direction η, we want to estimate the coverage by calculating the squared difference of the intensity between η and its neighbors, i.e. $\left|I(\eta)-I(\eta_i)\right|^2$. The coverage of η would spread out from η until the squared difference exceeds a user-defined threshold. Next, we generate a priority queue by sorting the coverage-weighted square of the intensity of each unit direction. Then we choose the appropriate candidate directions from this priority queue. The choosing rule here is intuitive. If the direction of the considered candidate falls within the range covered by the candidates that we previously select, we reject this candidate, and take next candidate from the priority queue into consideration. On the contrary, we accept the candidate to be one of the set of our initial guess. Figure 5.2 (c) illustrates the circumstance we have chosen two candidates, and (d) describes the accepted case (the yellow one) and rejected case (the magenta one) by our choosing rule. This process would continue until the number of the selected candidates exceeds a user-defined threshold. If the priority queue becomes empty before the process terminate, we would narrow the coverage threshold previously defined by user, and restart the process from step (b).

4.1.3 BRDF Representation using Scattered SRBFs

After the fitting process, we have represented the BRDF data with scattered SRBFs for each fixed outgoing direction:

$$\rho_{\omega_o}(\omega_i) \approx \sum_{k=1}^{\mathrm{K}} F_{\mathrm{k}} G(\omega_i \cdot \xi_k ; \lambda_k) \tag{8}$$

where $\rho_{\omega_o}(\omega_i)$ is the BRDF with a fixed outgoing direction ω_o, G is the SRBF kernel function, ξ_k is the center of basis on unit sphere, λ_k is the bandwidth of the basis, F_k is the basis coefficient, and K is the number of the bases.

Given an arbitrary viewing direction in 3D space, we need to compute the SRBFs composed of the SRBFs of neighbor outgoing directions. Then, the BRDF is given as:

$$\rho(\omega_i, \omega_o) \approx \sum_{n=1}^{N} W_n \sum_{k=1}^{K} F_k G(\omega_i \cdot \xi_k; \lambda_k), \tag{9}$$

where N is the number of neighbor directions. N would vary according to the given viewing direction. Its value would be 3 or 4 in usual. W_n is the weight for each SRBF expansion. The weight W_n is inversely proportion to the geodesic distance between the given direction and the neighbor outgoing direction. Using this representation we can easily generate samples for rendering with the multiple importance sampling technique. This will be discussed further in next section.

4.2 Run-Time Rendering Process

Importance sampling is a technique to reduce the image variance. Now we have represented the BRDF with the scattered SRBFs. Traditional importance sampling is to find a probability density function (PDF) which describes the density distribution of the entire data region, i.e. the hemisphere for BRDF. However, in this case, it's hard to combine the PDFs into a new one that describes the distribution of the sum of all related scattered SRBFs. On the other hand, we can't directly use the distribution function derived from each SRBF neither. It's because that each SRBF may overlap each other. It's only correct when all SRBFs are disjoint, and this will become another sampling technique named stratified sampling. Therefore, we apply an alternative approach presented by Veach and Guibas [21] - *multiple importance sampling*, which allows all sampling strata to overlap each other. Since each SRBF kernel can be taken as some kind of the density distribution function. Thus we can easily generate samples from each SRBF kernel. With the aid of multiple importance sampling, we can make the rendering process more efficient and compact when we use scattered SRBFs to represent BRDF.

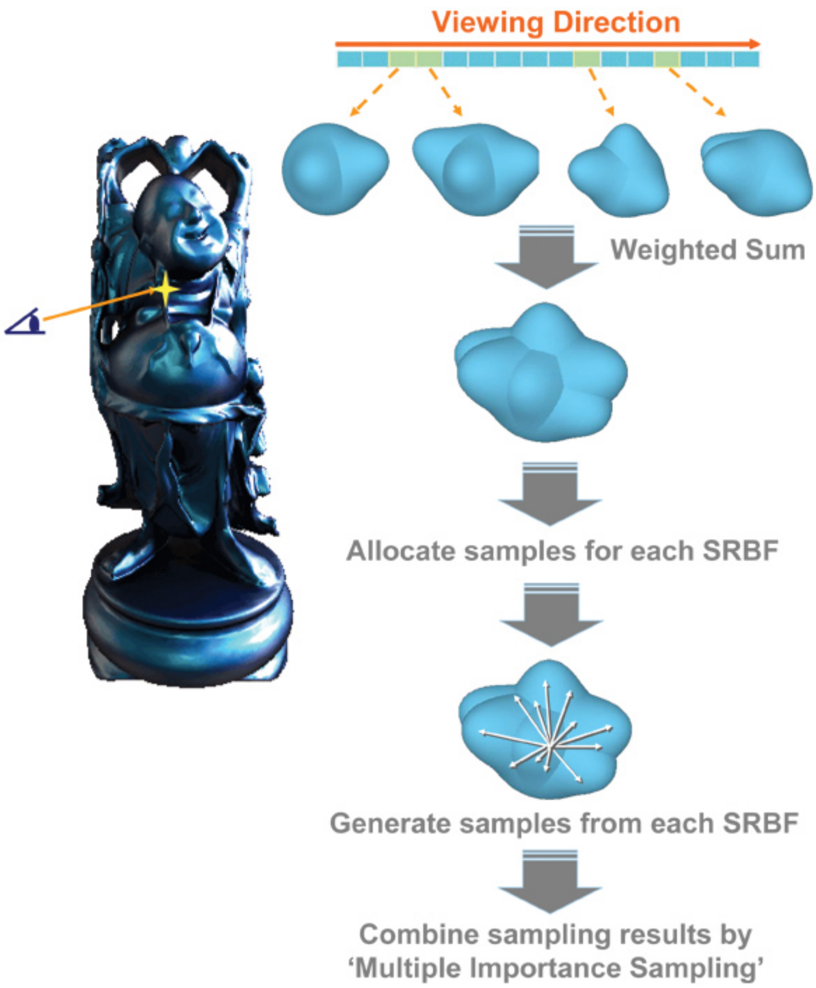

Figure 4.3: Run-Time Rendering Process

Figure 4.3 illustrates the flow of our rendering process. When the view ray hits the object in a scene, we first weight sum the SRBFs of three or four near fixed view direction that we construct in off-line process. Next, we determine the number of samples of each SRBF according to its integral. Then we generate samples from each SRBF and combine the results by multiple importance sampling technique.

In this section, we start by introducing the multiple importance sampling. We then describe how we determine the number of samples that should be taken from each SRBF, and how we generate sampling direction from each SRBF.

4.2.1 Multiple Importance Sampling

When tracing a path through the scene by BRDF importance sampling, it is desirable to generate rays distributed according to the density of BRDF. We are interested in evaluating the integral of the incident illumination for a fixed outgoing direction ω_o located at x with normal n,

$$\begin{aligned} &\int_\Omega L_i(x,\omega_i)\rho(x,\omega_i,\omega_o)(\omega_i \cdot n)d\omega_i \\ &\approx \frac{1}{n}\sum_{s=1}^{n} L_i(x,\omega_s)\left[\frac{\rho(x,\omega_i,\omega_o)}{\gamma(\omega_s \mid \omega_o)}\right](\omega_s \cdot n) \end{aligned} \tag{10}$$

where the first line is the reflection equation, and the second line is a Monte Carlo estimator for importance sampling. However, it's hard to construct a single PDF $\gamma(\omega_s \mid \omega_o)$ that follows the shape of the complex BRDF. There is an alternative technique for importance sampling presented by Veach and Guibas [21] called *multiple importance sampling*. This technique makes Monte Carlo integration more robust by combining several potentially good estimators. These estimators computed by different PDFs may have different qualities in different regions of the integration domain. Veach and Guibas make a weighted-average of all estimators where the weights depend on the sampling positions. If we want to evaluate the integral of f(x)

$$\int_\Omega f(x)dx,$$

and we have *n* different estimators, the combined estimator is then given by

$$F = \sum_{i=1}^{n} \frac{1}{n_i} \sum_{j=1}^{n_i} w_i(X_{i,j}) \frac{f(X_{i,j})}{p_i(X_{i,j})} \tag{11}$$

where p_i is the PDF for each estimator, n_i denotes the number of samples from p_i, $X_{i,j}$ are the samples from p_i, for $j = 1,...,n_i$, and all samples are assumed to be independent. w_i is the weighting function and satisfy the following two conditions:

$$\begin{cases} \sum_{i=1}^{n} w_i(x) = 1 \\ w_i(x) = 0 \ \textit{whenever} \ p_i(x) = 0 \end{cases}, \tag{12}$$

Then, the expected value of the combined estimator F would be equal to the integral of *f(x)* which we want to evaluate.

So far, we have represented the BRDF using scattered SRBFs. Now we apply this technique to BRDF importance sampling, and the Equation (10) would become:

$$\begin{aligned} &\int_{\Omega} L_i(x,\omega_i)\rho(x,\omega_i,\omega_o)(\omega_i \cdot n)d\omega_i \\ &\approx \sum_{i=1}^{n} \frac{1}{n_i} \sum_{j=1}^{n_i} \left(\frac{n_i p_i(X_{i,j})}{\sum_k n_k p_k(X_{i,j})} \right) L_i(x, X_{i,j}) \left(\frac{\rho(x, X_{i,j}, \omega_o)}{p_i(X_{i,j})} \right) (X_{i,j} \cdot n) \end{aligned} \tag{13}$$

where *n* is the number of SRBFs, n_i denotes the number of samples from each SRBF, and p_i is the PDF calculated from each SRBF kernel, for $i = 1,...,n$. $X_{i,j}$ are the samples from each SRBF kernel, for $j = 1,...,n_i$.

Now, there are two issues: one is how to determine n_i, the number of samples should be taken from each SRBF kernel, the other is how to generate $X_{i,j}$, the sampling directions distributed according to each SRBF kernel. These will be discussed in the following subsection.

4.2.2 Sampling Algorithm

We now describe how to use our representation for multiple importance sampling. Intuitively, each scattered SRBF covers a part of the entire BRDF region. Although there would be two or more SRBFs overlap in some regions, we can still gather the intensity of multiple sampling directions within a pixel using *multiple importance sampling* approach.

As mentioned before, we fit scattered SRBFs to the data in the vector of each discrete outgoing direction respectively. At run time, for a given viewing direction, we need to combine the scattered SRBFs of three or four nearest viewing directions. Then, we have multiple SRBF kernel functions, now we should decide how many samples should be taken from each SRBF kernel. Let's recall that SRBF is defined on the unit sphere, and its integral is easy to be calculated by using the *spherical singular integral* property of SRBF. The integral of each SRBF can be taken as its total energy gathered from all directions. Therefore, it's straightforward to allocate samples according to the ratio of the integral of each SRBF to the sum of all SRBFs' integrals. The probability of choosing the SRBF l for each sample is given by:

$$P(l) = \frac{I_l}{\sum_{i=1}^{n} I_i} \tag{14}$$

We calculate a 1D CDF over l from these probabilities. In the dispatching process, we generate a uniform random variable in [0, 1] for each sample, and traverse the CDF to determine where the sample should be taken from.

Next, we generate a sample direction in each SRBF kernel by sequentially selecting the elevation angle θ and the azimuth angle φ defined on the plane whose normal is parallel with the SRBF kernel's center (Figure 4.4).

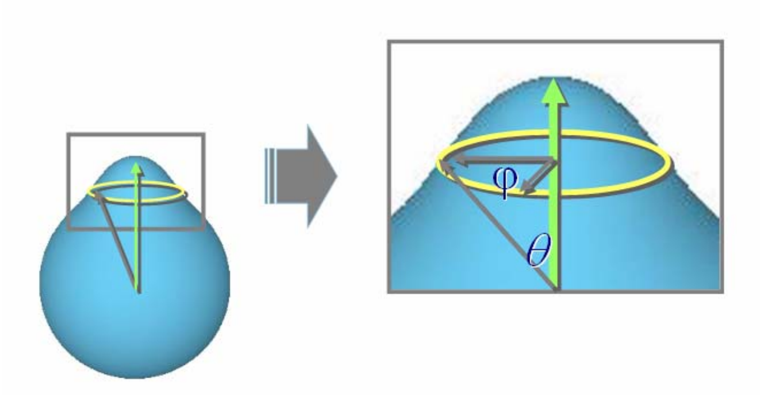

Figure 4.4: The elevation angle θ and the azimuth angle φ defined against SRBF.

Having chosen the SRBF basis to sample, we can consider its PDF proportion to its kernel function. With the kernels easy for integration and inversion, such as Gaussian kernel, we can use the *inversion method* to generate random samples directly. We first normalize the kernel function to get a PDF $p(x)$, since the integral of PDFs over their domain should equal to 1. After integrating $p(x)$, we can get the cumulative distribution function (CDF) $P(x)$. Then, we calculate the inverse of CDF $P^{-1}(x)$, and generate a uniformly distributed random number ξ in [0, 1] to evaluate the $P^{-1}(x)$. We can easily get the elevation angle θ of the sampling direction.

On the other hand, for the kernel which is hard to apply inversion method, we can use *metropolis random walk algorithm* to generate samples with a desired density instead. It should be noted that the SRBF kernel itself only describes 1D density, while the desired density for sampling is the density over the sphere. Therefore, when we select the elevation angle θ by this approach, we should consider the influence of the circumference around the center of SRBF kernel especially.

The azimuth angle φ defined in each SRBF is easy to be calculated. Because each SRBF kernel is symmetric against the vector that defined by its center and the origin of the unit sphere. Therefore, the distribution of azimuth angle φ is uniform, and we can simply generate a random number in $[0, 2\pi]$ to evaluate φ. With SRBF center, θ and φ, we can simply get the sampling direction by two rotation operations.

Chapter 5

Implementation and Results

This chapter demonstrates the results in three aspects. First, we will examine the fitting errors when we use scattered SRBFs to represent the BRDF data measured by the Cornell University [5]. We wound compare our model with Lafortune model [10]. Then, we take a look at the distributions of samples to show how close those samples are generated with desired density. Here, we would compare two random sample generating methods, one is the *inversion method*, and the other is the *metropolis random walk algorithm*. Finally, we illustrate the rendering results of four different measured BRDF data and several complex scenes.

5.1 Fitting Errors

We now compare the fitting performance between Lafortune model and our SRBF representation. Lafortune model [10] which combines multiple generalized cosine-lobes can be written as:

$$\rho(u,v) = \sum_i (C_{x,i}u_x v_x + C_{y,i}u_y v_y + C_{z,i}u_z v_z)^{n_i} \qquad (15)$$

where u is the incident direction, v is the outgoing direction. In this fitting process, they apply a non-linear optimization technique to determine the parameters

C_x, C_y, C_z *and* n_i. The objective is to minimize the mean-square error of the reflectance functions multiplied by the cosines of the incidence angles with the normal. Because they fit the model depending on the outgoing and incident directions at the same time, it is not easy to figure out the initial guess. Consequently, it is sometimes hard to fit their model to some complex measured BRDF data.

	Lafortune model	Scattered SRBFs
Paint Blue	32%	14%
Garnet Red	7.6%	4%
Krylon Blue	10%	5.9%
Cayman	19%	5.9%

Table5.1: The comparison of fitting errors.

Table 5.1 displays the fitting errors of Lafortune model and the scattered SRBFs representation with Gaussian SRBF kernels. (These four different materials in Table 5.1 are measured by Cornell University [5]). Since it's hard to find a good strategy of initial guess for complex BRDF data when fitting the Lafortune model, we randomly generate the initial guesses and execute the fitting process lots of times (100 times for each BRDF). In our experiments, we found although we add the number of lobes for Lafortune model, it's still hard to improve the fitting performance. We compare our results with the best-fit Lafortune models (with 3 lobes) finally.

5.2 Sampling

In this section, we will examine the sampling distributions according to our sampling algorithm. As mentioned in Section 4.2.2 there are two approaches to generate random samples from each SRBF. Here, we compare these two methods. When using metropolis random walk algorithm to choose a random sample, we assume some preconditions. For computational efficiency, we only take few steps for each sampling direction (in Figure 5.1, we take five steps for each sample) and we constrain the evaluated value in the range of random walking must be greater than 0.01. With these preconditions, we can use metropolis random walk algorithm to generate sampling directions which are similar to those generated by the inversion method. Figure 5.1 illustrates the sampling distributions of 50, 100, 300, and 600 samples generated by these two generating algorithms with scattered SRBFs representation.

From Figure 5.1, we can see that the distributions resulting from these two methods are very similar. This makes our sampling scheme more flexible on the basis of scattered SRBFs representation. Our sampling method can be applied not only to the kernels easy for inversion but also to the kernels hard to inverse their integral. We can choose an appropriate method to generate samples according to the intrinsic properties of SRBF kernels.

(a) Inversion 50 samples

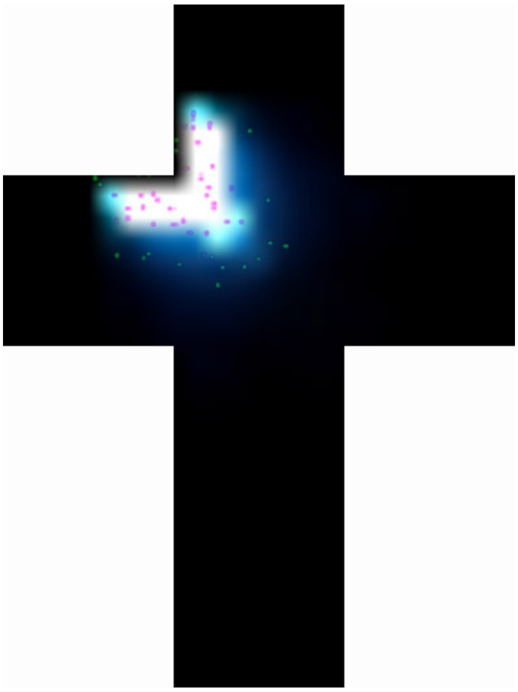

(b) Metropolis 50 samples

(c) Inversion 100 samples

(d) Metropolis 100 samples

(e) Inversion 300 samples

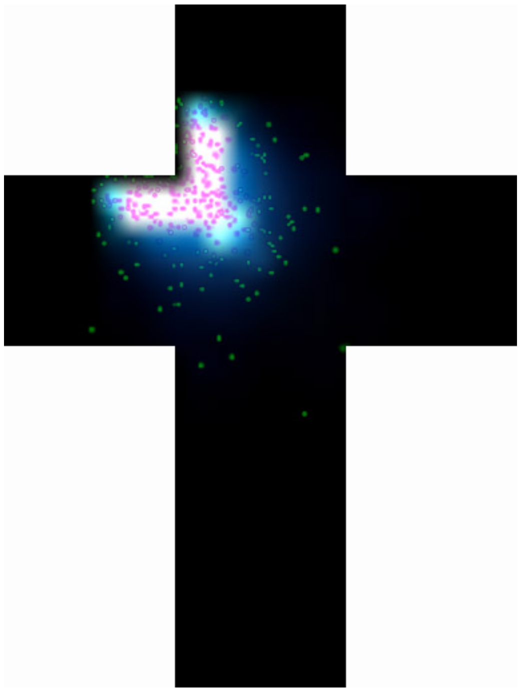

(f) Metropolis 300 samples

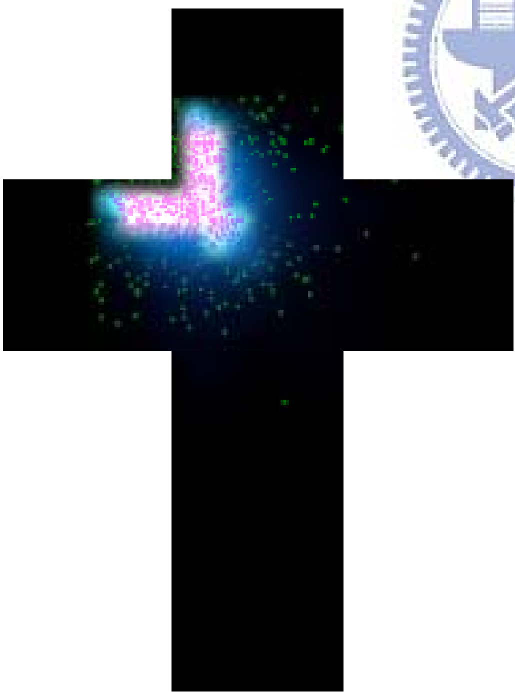

(g) Inversion 600 samples

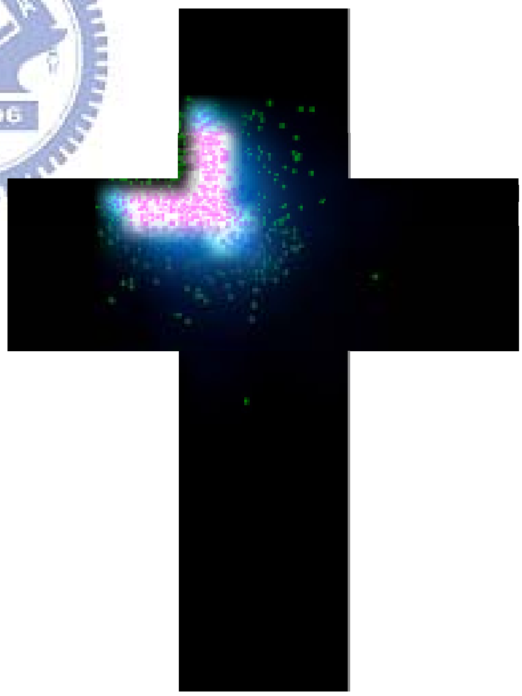

(h) Metropolis 600 samples

Figure 5.1: Comparison of sampling distributions between inversion method and metropolis random walk algorithm.

5.3 Rendering

We now illustrate the rendering results of BRDF importance sampling. In order to avoid the influence of visibility and complex illumination, we render the images of a sphere lit by an environment map in 32-bit ARGB pixel format for quantitative comparisons. We render the sphere with four different materials which are measured by Cornell University [5]. Figures 5.2~5.5 are the comparisons between Lafortune sampling method and our SRBFs sampling method where samples are generated by inversion method. In general, there are two main factors that affect the image qualities, one is the fitting errors of the representing form of BRDF data, and the other is the sampling algorithm for that representation. In the phase of sampling algorithm, both Lafortune sampling method and ours use the basis functions as the density functions directly, thus the generated samples distribute with the desired densities nearly exactly. Therefore, the differences from images in Figures 5.2~5.5 mostly result from the differences in the fitting qualities of those two representations.

We also render several images of a complex scene. We represent each BRDF measurements in scattered SRBFs with 12 Gaussian kernels. The samples within each pixel are generated by inversion method. For each different material, we choose its best-fit Lafortune model with 3-lobes for rendering comparison. Figure 5.6 contains a 'Krylon Blue' teapot and a 'Paint Blue' plane in the 'Funston Beach' environment [http://www.debevec.org/Probes/]. In Figure 5.7, there is a 'Cayman' Buddha placed on 'Garnet Red' plane in front of 'Uffizi Gallery'. From these two rendering results, we can find that the results of our method with 300 samples equal to or better than those of Lafortune sampling with 1200 samples.

(a) SRBF sampling (100 samples)

(b) SRBF sampling (300 samples)

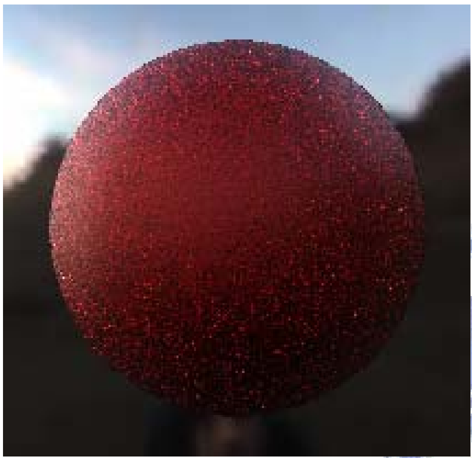

(c) Lafortune sampling (100 samples)

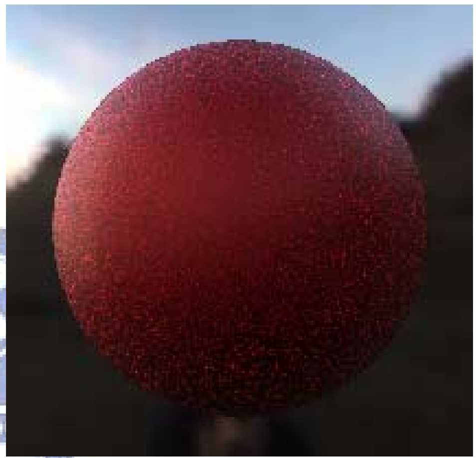

(d) Lafortune sampling (300 samples)

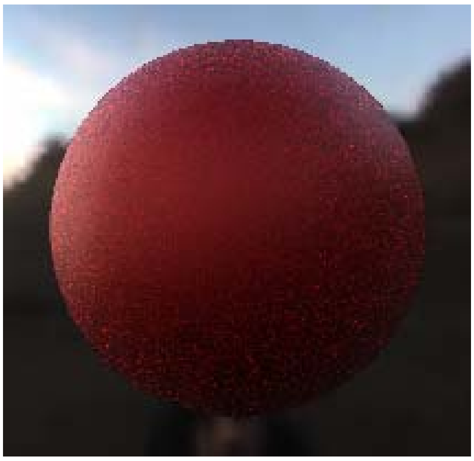

(e) Lafortune sampling (600 samples)

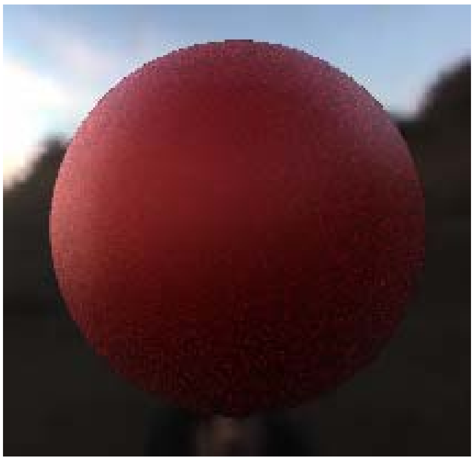

(f) Lafortune sampling (1200 samples)

Figure 5.2: Sampling Results with material ‘Garnet Red’

(measured by Cornell University)

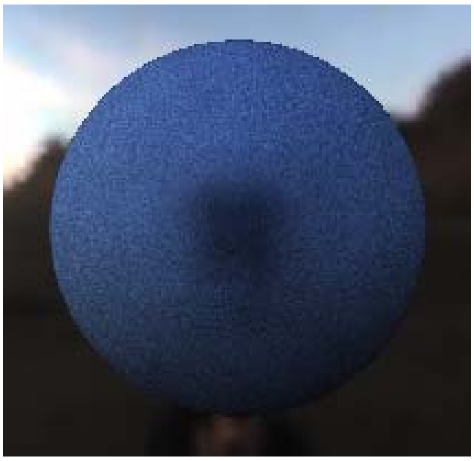

(a) SRBF sampling (100 samples)

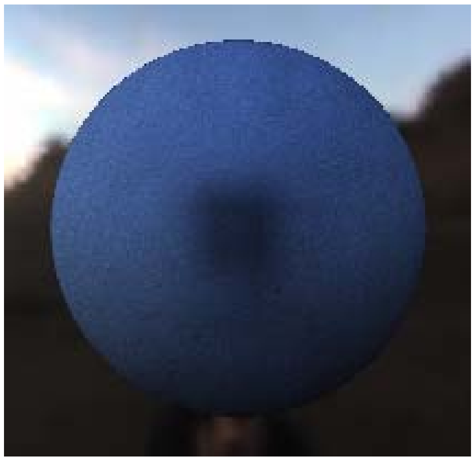

(b) SRBF sampling (300 samples)

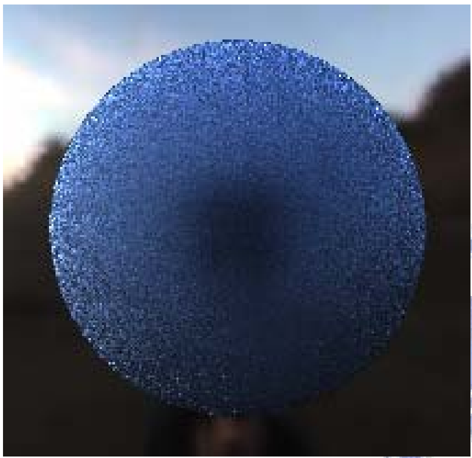

(c) Lafortune sampling (100 samples)

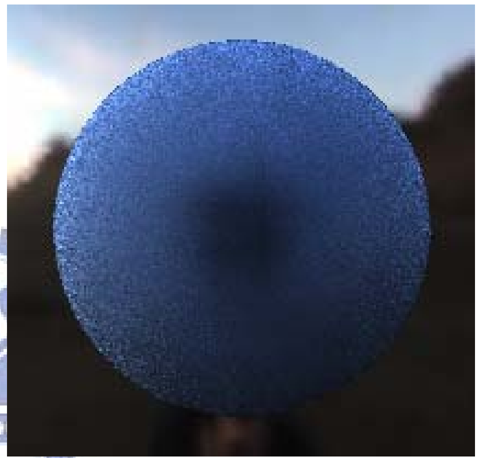

(d) Lafortune sampling (300 samples)

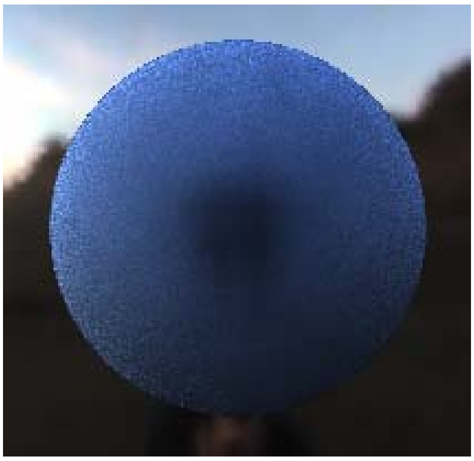

(e) Lafortune sampling (600 samples)

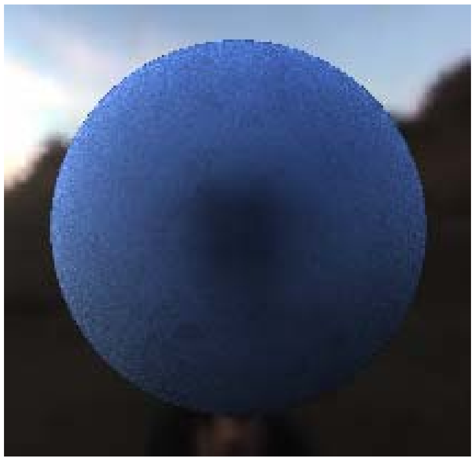

(f) Lafortune sampling (1200 samples)

Figure 5.3: Sampling Results with material ‘Paint Blue’

(measured by Cornell University)

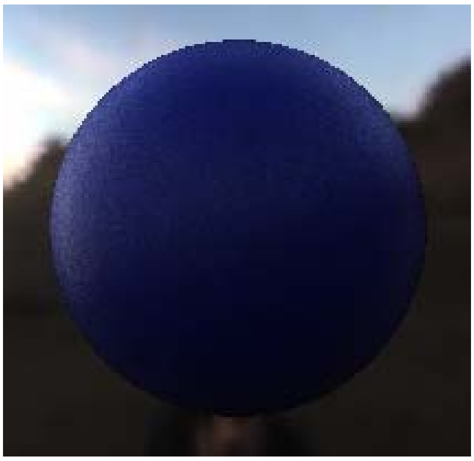

(a) SRBF sampling (100 samples)

(b) SRBF sampling (300 samples)

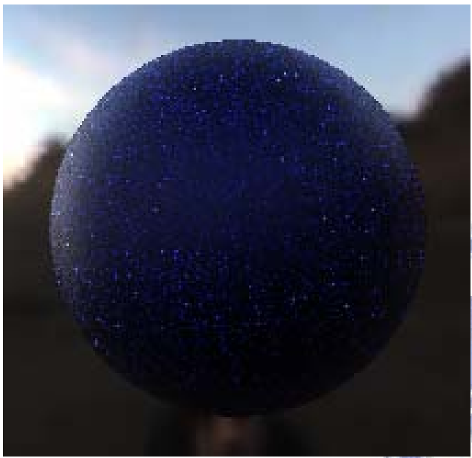

(c) Lafortune sampling (100 samples)

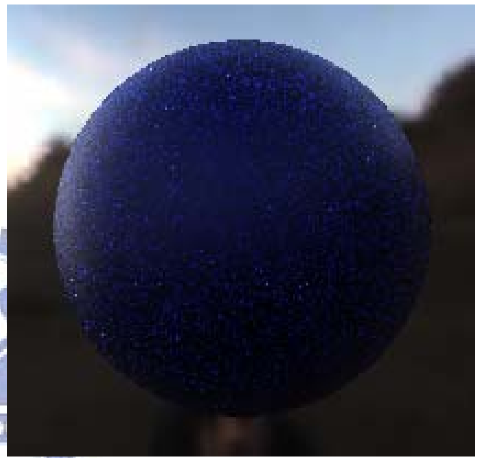

(d) Lafortune sampling (300 samples)

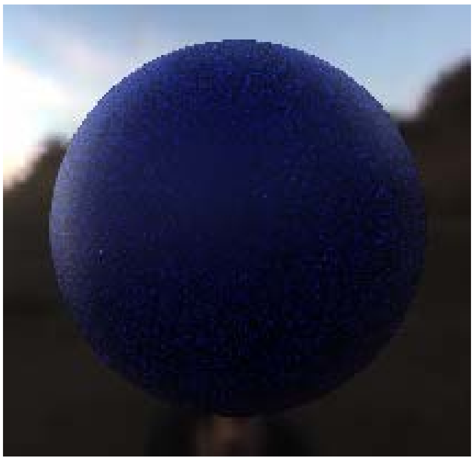

(e) Lafortune sampling (600 samples)

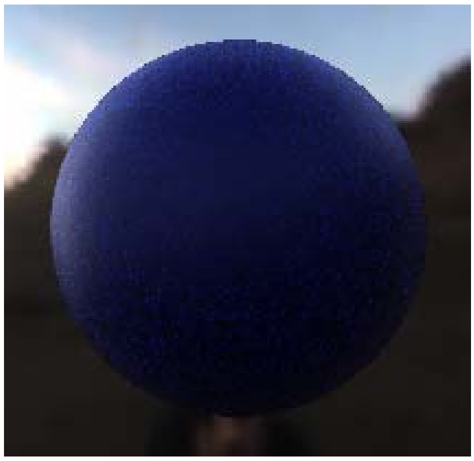

(f) Lafortune sampling (1200 samples)

Figure 5.4: Sampling Results with material ‘Krylon Blue’

(measured by Cornell University)

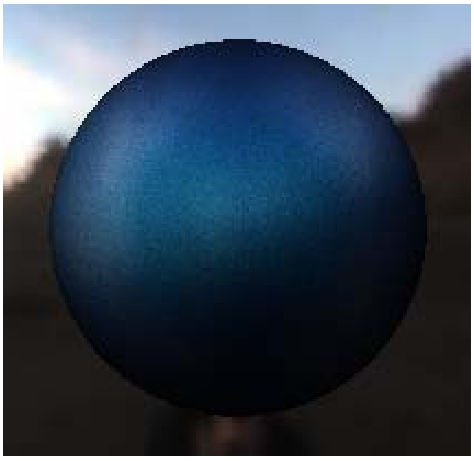

(a) SRBF sampling (100 samples)

(b) SRBF sampling (300 samples)

(c) Lafortune sampling (100 samples)

(d) Lafortune sampling (300 samples)

(e) Lafortune sampling (600 samples)

(f) Lafortune sampling (1200 samples)

Figure 5.5: Sampling Results with material ‘Cayman’

(measured by Cornell University)

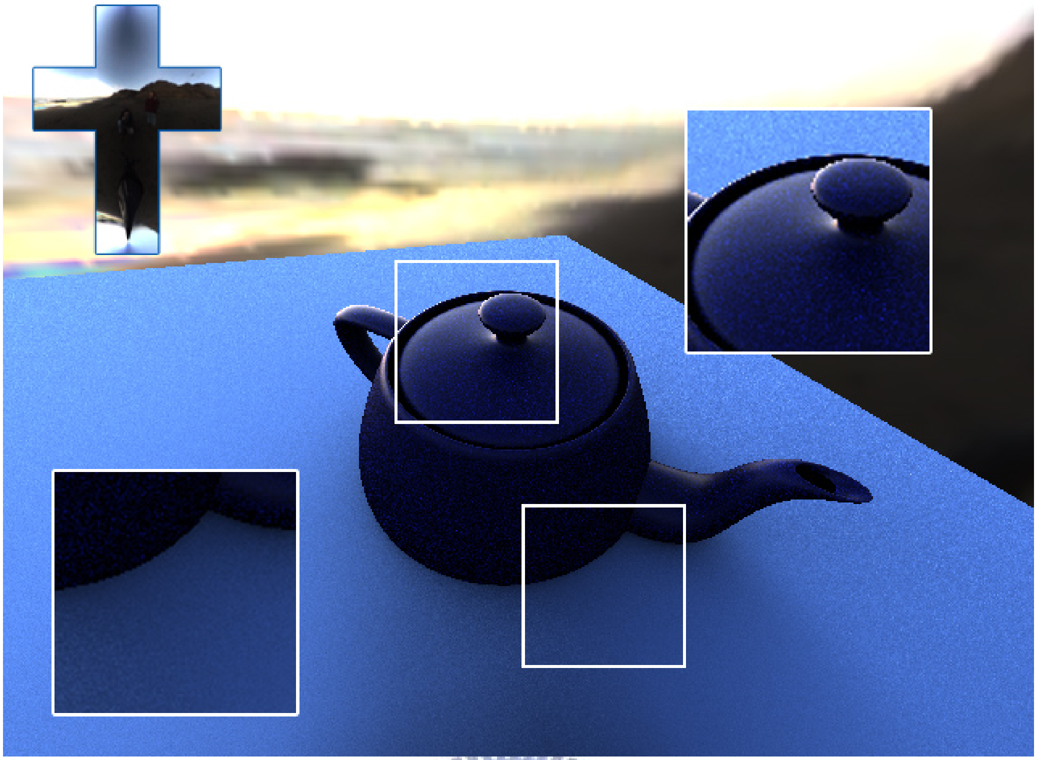

(a) Lafortune sampling (1200 samples/pixel)

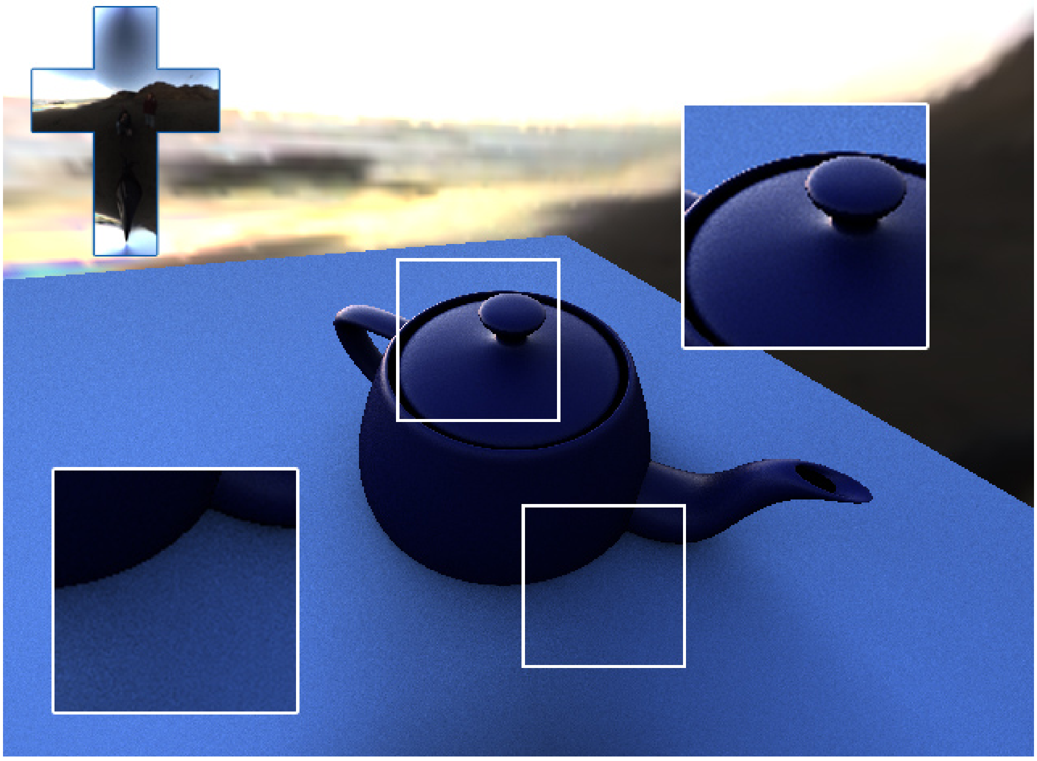

(e) SRBF sampling (300 samples/pixel)

Figure 5.6: ‘KrylonBlue’ teapot on the ‘PaintBlue’ plane in the ‘Funston Beach’ HDR environment.

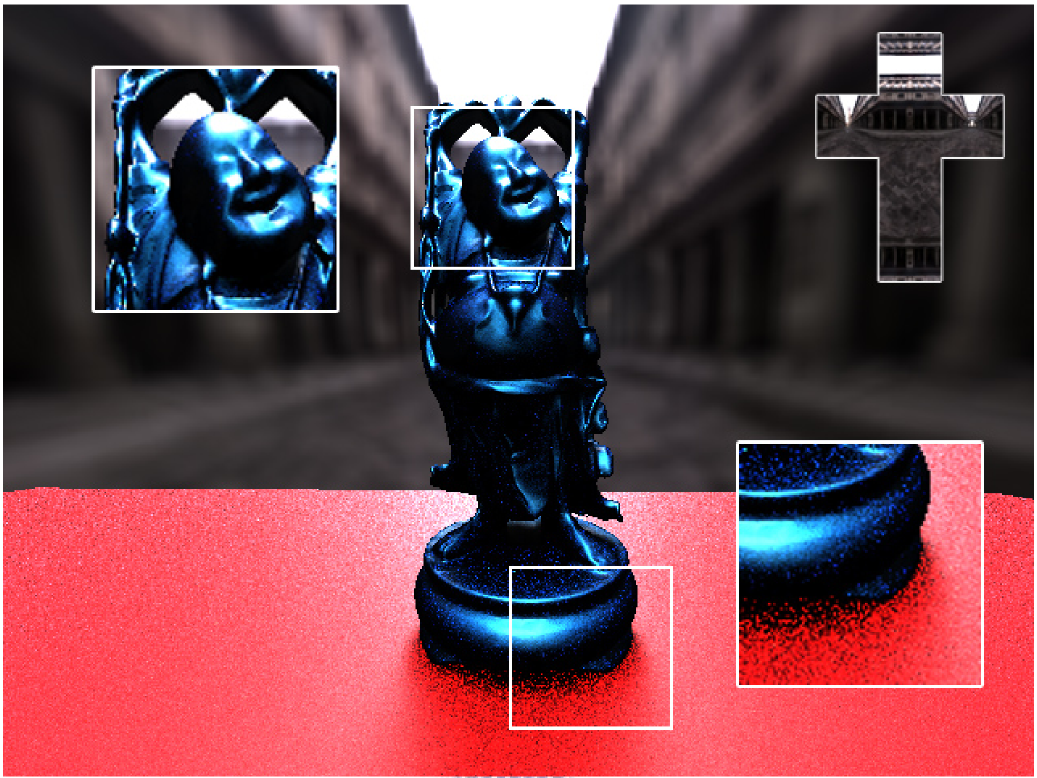

(a) Lafortune sampling (1200 samples)

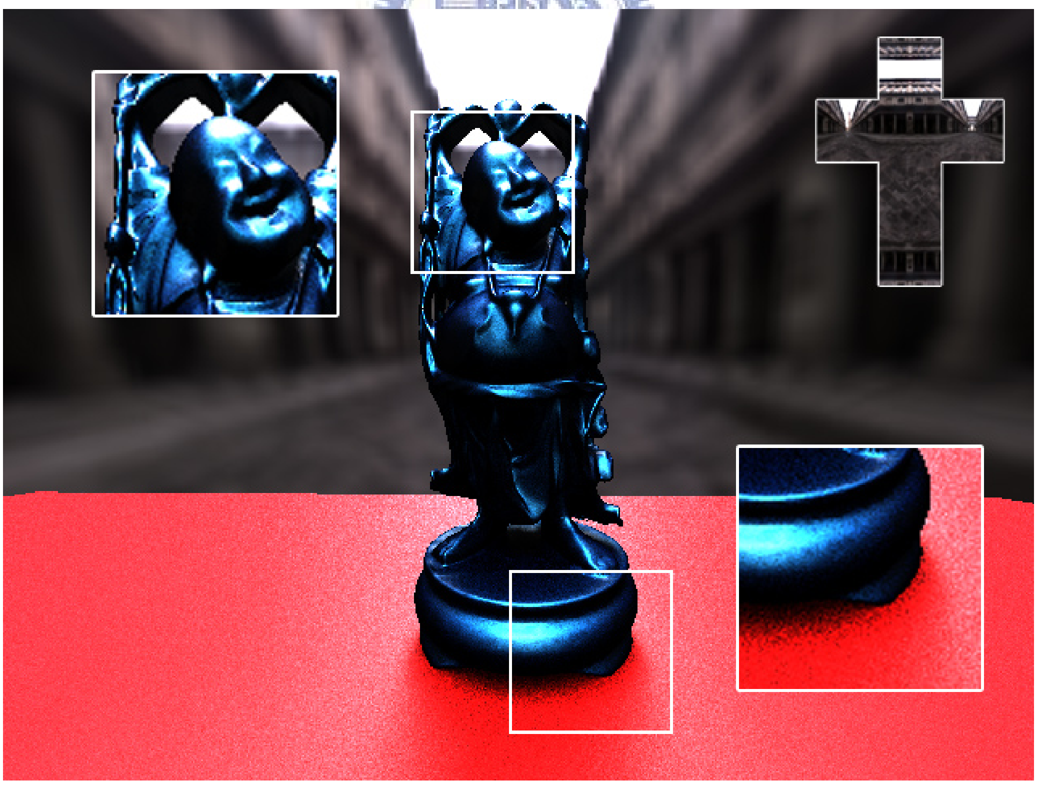

(b) SRBF samplings (300 samples)

Figure 5.7: A 'Cayman' Buddha and a 'GarnetRed' plane
in 'Uffizi Gallery' HDR environment

Chapter 6

Conclusions and Future Works

In this thesis, we introduce a novel representation of BRDF by using scattered SRBFs. We express that the modified fitting algorithm also performs well with the measured BRDF data. Based on the scattered SRBFs representation, we can generate samples following the desired densities efficiently. The random samples of each SRBF kernel can be generated efficiently not only by the inversion method but also by the metropolis random walk algorithm. Furthermore, this BRDF representation is easy to be applied to the *multiple importance sampling* technique. Finally, we use our sampling scheme to render scenes with multiple complex materials with global illumination and shadows.

Our method so far can't deal with the complex HDR lighting environment, because we consider the importance of BRDF data only. If the lighting environment is complex and the intensity within each pixel change dramatically, the illumination would become the dominant factor that affects the image variance. In future work, we would like to extend our sampling scheme to analyze the product of BRDF and lighting environment. Since SRBFs have some great properties for this application, such as spherical singular integral, rotation invariant, etc, we are probably able to estimate the densities and generate samples at run-time. Although the computation time of density estimations would increase, we can generate much smaller samples than the approach considering BRDF only to get the same rendering quality. Because the major computation cost for ray tracing is the visibility testing, if we could generate samples smarter, we would improve the efficiency of importance sampling. Estimating the densities of the product of BRDF and lighting environment may make the sampling process more efficient in global illumination.

Reference

[1] Agarwal, S., Ramamoorthi, R., Belongie, S., and Jensen, H. W. 2003. Structured Importance Sampling of Environment Maps. ACM Transactions on Graphics 22, 3, 605–612.

[2] Claustres, L., Paulin, M., and Boucher, Y. 2003. BRDF Measurement Modelling using Wavelets for Efficient Path Tracing. Computer Graphics Forum 22, 4, 701–716.

[3] Cohen, J., and Debevec, P., 2001. LightGen, HDRShop plugin. http://www.ict.usc.edu/ jcohen/lightgen/lightgen.html.

[4] Cook, R. L., and Torrance, K. E. 1982. A reflectance model for computer graphics. ACM Trans. Graph. 1, 1, 7-24.

[5] The Cornell University Program of Computer Graphics - Reflectance Data. Web page. http://www.graphics.cornell.edu/online/measurements/reflectance/index.html.

[6] Freeden, W., Gervens, T., and Schreiner, M. 1998. Constructive Approximation on the Sphere. Oxford University Press.

[7] He, X. D., Torrance, K. E., Sillion, F. X., and Greenberg, D. P. 1991. A comprehensive physical model for light reflection. In *SIGGRAPH* 91, 175-186.

[8] Kajiya, J. T. 1986. The Rendering Equation. In *SIGGRAPH* 86, 143–150.

[9] Kollig, T., and Keller, A. 2003. Efficient Illumination by High Dynamic Range Images. In Eurographics Symposium on Rendering, 45–50.

[10] Lafortune, E. P. F., Foo, S.-C., Torrance, K. E., and Greenberg, D. P. 1997. Non-Linear Approximation of Reflectance Functions. In *SIGGRAPH* 97, 117–126.

[11] Lafortune, E. P., and Willems, Y. D. 1994. Using the modified Phong reflectance model for physically based rendering. Technical Report RP-CW-197, Department of

Computing Science, K.U. Leuven, 1994. 1

[12] Lalonde, P. 1997. Representations and Uses of Light Distribution Functions. PhD thesis, University of British Columbia.

[13] Lawrence, J., Rusinkiewicz, S., and Ramamoorthi, R. 2004. Efficient BRDF Importance Sampling using a Factored Representation. ACM Transactions on Graphics 23, 3, 496–505.

[14] Matusik, W., Pfister, H., Brand, M., and McMillan, L. 2003. A Data-Driven Reflectance Model. ACM Transactions on Graphics 22, 3, 759–769.

[15] Narcowich, F. J., AND Ward, J. D. 1996. Nonstationary Wavelets on them-Sphere for Scattered Data. Applied and Computational Harmonic Analysis 3, 4, 324–336.

[16] Pharr, M., and Humphreys, G. 2004. Physically Based Rendering: From Theory to Implementation. Morgan Kaufmann.

[17] Phong, B. T. 1975. Illumination for computer generated pictures. Commun. ACM 18, 6, 311-317.

[18] Rusinkiewicz, S. M. 1998. A New Change of Variables for Efficient BRDF Representation. In Eurographics Workshop on Rendering, 11–22.

[19] Shirley, P. S. 1991. Physically Based Lighting Calculations for Computer Graphics. PhD thesis, University of Illinois at Urbana-Champaign.

[20] Tsai, Y. T., and Shih, Z. C. 2006. All-Frequency Pre-computed Radiance Transfer using Spherical Radial Basis Functions and Clustered Tensor Approximation. *SIGGRAPH* 06, accepted.

[21] Veach, E., and Guibas, L. 1995. Optimally combining sampling techniques for Monte Carlo rendering. In *SIGGRAPH* 95, 419-428.

[22] Ward, G. J. 1992. Measuring and modeling anisotropic reflection. In *SIGGRAPH* 92, 265-272.

[23] Zhu, C., Byrd, R. H., Lu, P., and Nocedal, J. 1997. Algorithm 778: L-BFGS-B: Fortran Subroutines for Large-Scale Bound-Constrained Optimization. ACM Transactions on Mathematical Software 23, 4, 550–560.